

Tennessee State University

Digital Scholarship @ Tennessee State University

Information Systems and Engineering
Management Research Publications

Center of Excellence in Information Systems
and Engineering Management

9-1993

SPOT on RS CVn From Spectroscopy and Photometry

Joel A. Eaton

Tennessee State University

Gregory W. Henry

Tennessee State University

Coretta Bell

Tennessee State University

Albert Okorogu

Tennessee State University

Follow this and additional works at: <https://digitalscholarship.tnstate.edu/coe-research>



Part of the [Stars](#), [Interstellar Medium and the Galaxy Commons](#)

Recommended Citation

Eaton, J.A.; Henry, G.W.; Bell, C.; Okorogu, A. "SPOT on RS CVn From Spectroscopy and Photometry"
Astronomical Journal v.106, p.1181 (1993)

This Article is brought to you for free and open access by the Center of Excellence in Information Systems and Engineering Management at Digital Scholarship @ Tennessee State University. It has been accepted for inclusion in Information Systems and Engineering Management Research Publications by an authorized administrator of Digital Scholarship @ Tennessee State University. For more information, please contact XGE@Tnstate.edu.

SPOTS ON RS CVn FROM SPECTROSCOPY AND PHOTOMETRY

JOEL A. EATON,¹ GREGORY W. HENRY, CORETTA BELL, AND ALBERT OKOROGU

Center of Excellence in Information Systems, Tennessee State University, Nashville, Tennessee 37203

Electronic mail: eatonja@ctrvax.vanderbilt.edu, henry@tsu.bitnet

Received 1993 April 16; revised 1993 May 25

ABSTRACT

We have used contemporaneous spectra and V light curves to form spot models for RS CVn in 1991 and 1992. More than two spots are needed to fit all the properties of the observations. In fact, moderately small spots (22×28 deg in latitude and longitude) having only a slight effect on the rotational light curve were eclipsed in both years, and we find that a collection of 6–8 such moderate spots is required to fit the line profiles in each year. These groups of spots also account naturally for a difference in level of light between the two years. There is no evidence for polar spots larger than ~ 18 degrees in radius. We have also derived new orbits from radial velocities of the stars, which give the mass ratio $M_1/M_2 = 1.04 \pm 0.02$.

1. INTRODUCTION

Hall (1976) identified a group of binary stars with a chromospherically active subgiant component that vary by several tenths of a magnitude as they rotate. He argued that the light variation is caused by large dark spots on the subgiant's surface and named the class for RS Canum Venaticorum. Observations in temperature-sensitive lines, such as TiO bands, show that the spots of these RS CVn binaries are considerably cooler than the surrounding photosphere (Ramsey & Nations 1980). Eclipses of spots confirm this result (Eaton 1991). Distortions of spectral line profiles by spots also find dark spots and, if well enough observed, locate the spots uniquely on the star (Vogt & Penrod 1983).

Analysis of photometry alone has found truly huge spots on these stars. RS CVn, for example, may have spots so big that they extend up to about 76 degrees in angular diameter (Kang & Wilson 1989) over a star $4.1 R_\odot$ in radius. Analyses of many noneclipsing systems show that the light variation can usually be represented at any time by two large spots, or stable groups of spots, which rotate at slightly different rates, presumably because they are at different stellar latitudes, and which persist for an average of two years (Hall & Henry 1993; Henry *et al.* 1993). Whether these are large single spots, bipolar pairs, or larger groups of moderately sized spots is not yet clear. We have observed RS CVn to begin to address this question.

We are combining optical spectra and photoelectric photometry of RS CVn to determine the properties of its spots. In an analysis of the noneclipsing binary UX Ari, Noah *et al.* (1987) have shown that combining line profiles and light curves makes it possible to constrain spot solutions much better than using profiles or light curves alone. We shall apply this technique to the quintessential *eclipsing* system, RS CVn. Observing an eclipsing system is advantageous because the orbital inclination and radii of the

stars may be well known, and the inclination is usually close to 90 degrees. There is also the possibility that a spot will be eclipsed, which restricts its location and size dramatically. The disadvantage for a star like RS CVn, versus the systems like AR Lac and V711 Tau that are usually studied spectroscopically, is that the hot, unspotted component contributes a significant fraction of the light in the composite spectrum, about 55% in the red for RS CVn. Another disadvantage of eclipsing systems is that latitudes of spots are harder to determine than in systems with small inclinations, which display roughly a single hemisphere for our view. In eclipsing systems, spots at high latitude are always severely foreshortened, and there is a north–south ambiguity in the spots found.

We have chosen to observe the classical system RS CVn because it has a well-defined light curve. Historically, the rotational modulation of its light has implied that an exceptionally large area of the cool component is spotted. Total eclipses define the geometry of the system quite well (Eaton & Hall 1979; Kang & Wilson 1989), and eclipses of the spots themselves have been detected occasionally (Eaton & Hall 1979; Eaton 1991). Strassmeier & Fekel (1990) have classified the stars F6 IV and G8 IV by fitting red spectra with combinations of standard stars of various spectral types. These are somewhat different than the previous values, F5 IV and K0 IV (Strassmeier *et al.* 1988). Popper (1988) has obtained a recent orbit based on coude spectra.

We shall discuss the new observations in Sec. 2, obtain a new spectroscopic orbit from our radial velocities in Sec. 3, and derive spot solutions in Sec. 4. We have found that a reasonable solution of the light curve, based on a minimum number of spots, does not reproduce the observed line profiles, that a combination of 6–8 spots is required. In Sec. 5, we consider the implications of this, discuss the use of cross-correlation functions to define the blended line profiles of binary systems, and explore the possibility that the cool star has extensive polar spots. Section 6 summarizes our results.

¹Visiting observer at the National Solar Observatory.

2. OBSERVATIONS

The observations analyzed consist of *BV* photometry taken with the Vanderbilt/TSU robotic telescope and 70 high-dispersion spectra obtained with the McMath–Pierce Solar Telescope.

The Vanderbilt/TSU robotic telescope is a 16 in. computer-controlled telescope designed to obtain photoelectric photometry automatically (Genet *et al.* 1987). Normally, it is programed to observe a variable star once a night, but we can direct it to monitor a variable star on any given night. In this mode, it alternates between the variable and a comparison star (HD 114778 for RS CVn) as long as the variable is within a specified range of hour angle, observing a check star (HD 115197 for RS CVn) every tenth observation of the variable. We have observed parts of three primary and four secondary minima in 1991, three primaries and three secondaries in 1992. Data for phases outside the eclipses were collected in the normal mode of one observation (three integrations for the variable, four for the comparison) per night. All the data have been corrected for the estimated dead time of the photomultiplier and for differential atmospheric extinction, and they have been transformed to the *UBV* system. Figure 1 shows the visual light curves for 1991 and 1992. They contain 1471 observations for 1991 and 1375 for 1992; a similar number exist for the *B* band. Between the 1991 and 1992 seasons we replaced the photometer with a new precision photometer that uses a CCD camera for quick and precise centering of stars in the diaphragm (Henry & Hall 1993). This change led to a reduction of the scatter of the data from $\sigma=0.008$ mag per point to 0.005 in both *V* and *B* (outside primary eclipse). The improvement should be apparent in the observations for secondary eclipses in Figs. 1 and 7.

We have obtained two new times of minimum light from these observations, HJD 2 448 379.1993 \pm 0.0001 and HJD 2 448 729.4310 \pm 0.0001. Combined, they yield the following new ephemeris:

$$\text{HJD}(\text{Obs.}) = 2\,448\,379.1993 + 4.797695 \cdot \text{Phase}, \quad (1)$$

which we have used through our analysis.

The 70 spectra of RS CVn are identified in Table 1. We obtained 70 other spectra of roughly 30 comparison stars to use as velocity standards and for simulating the composite spectra of RS CVn. These observations were made in runs covering 1991 April 25–30 and 1992 April 19–24 with the stellar spectrograph of the McMath–Pierce solar telescope at the National Solar Observatory. Spectra were recorded in the 6400–6480 Å range at a dispersion of 0.096 Å/pixel. The resolution (full width at half maximum) is roughly 1.7 pixels, or 0.16 Å. The exposure time for RS CVn was typically 40 min. Listed in the table are the date of observation (UT month/day/year), heliocentric Julian date, orbital phase, and the measured radial velocities of the two stars.

Figure 2 gives sample spectra for RS CVn and several comparison stars. The comparisons α CMi (F5 IV) and κ CrB (K1 IV) are the ones we have chosen to use to represent the components of RS CVn. The star HR 3639 is an

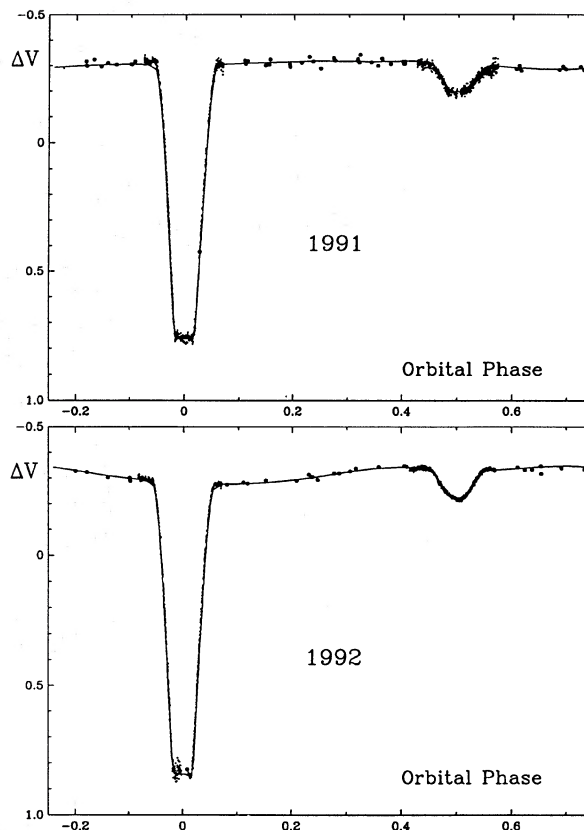


FIG. 1. Light curves for RS CVn in 1991 and 1992. Data are plotted as ΔV vs the orbital phase of Eq. (1). Individual data in the eclipses are represented as small dots; nightly means outside eclipse, as large dots. The solid curves represent reasonable three-spot solutions that do not adequately reproduce the line profiles, as discussed in Sec. 4. Geometrical elements are a combination of solutions by Eaton & Hall (1979) and Kang & Wilson (1989)—mostly Kang and Wilson—and were not reconverged to fit the light curves. Consequently, the solution does not fit primary minimum as well as it might.

M star with an effective temperature somewhat lower than the expected effective temperature of the spots, 3100–3450 K (Eaton 1991), which gives some idea of the contribution of spots to the line profiles. All three of these stars have sharp lines for their spectral types; κ CrB, in particular, has lines at least as sharp as those in spectra of β Gem, α Boo, and HR 5847, among others.

3. RADIAL VELOCITIES FROM THE NEW SPECTRA

Spectra of RS CVn are blends of spectra of a sharp-lined F6 IV star and a rather highly rotationally broadened G8 IV star. Because of the noise in our data, we decided to use cross correlations between the observed composite spectra of RS CVn and spectra of slowly rotating stars of appropriate spectral types to determine the radial velocities and surface brightnesses of the two components. The cross correlation has the form

$$\text{CORR}(\text{RV}) = \sum (1 - I_{\text{RS CVn}}) \times [1 - I_{\text{Std}}(\text{RV})] / N, \quad (2)$$

TABLE 1. Optical spectra of RS CVn.

UT Date	JD	Phase	RV _h	RV _c	UT Date	JD	Phase	RV _h	RV _c
	2,448,000+					2,448,000+			
4/26/1991	372.7036	0.6461	60.5	-75.9	5/01/1991	377.7096	0.6895	70.5	-96.9
	372.7265	0.6509	60.5	-75.9		377.7388	0.6956	71.5	-101.9
	372.7557	0.6569	64.5	-71.9		377.7679	0.7016	71.5	-97.9
	372.8237	0.6711	65.5	-75.9	4/20/1992	732.6830	0.6778	69.5	-89.9
4/27/1991	373.7077	0.8554	56.5	-81.9		732.7128	0.6840	71.5	-90.9
	373.7383	0.8617	55.5	-76.9		732.7438	0.6905	72.5	-92.9
	373.7681	0.8680	51.5	-75.9	4/21/1992	733.6788	0.8854	45.5	-68.9
	373.8681	0.8888	42.5	-70.9		733.7079	0.8914	43.5	-63.9
	373.8980	0.8950	42.5	-66.9		733.7871	0.9079	36.5	-57.9
	373.9279	0.9013	37.5	-64.9		733.8163	0.9140	33.5	-54.9
4/28/1991	374.7035	0.0629	-47.5	17.1		733.8503	0.9211	29.5	-50.9
	374.7334	0.0692	-52.5	22.1		733.8809	0.9275	25.5	-46.9
	374.7653	0.0758	-56.5	26.1		733.9114	0.9339	23.5	-41.9
	374.8167	0.0865	-61.5	31.1		733.9420	0.9402	19.5	-
	374.8459	0.0926	-65.5	31.1	4/22/1992	734.7044	0.0991	-65.5	39.1
	374.8757	0.0988	-66.5	35.1		734.7350	0.1055	-69.5	40.1
	374.9063	0.1052	-70.5	35.1		734.7648	0.1117	-70.5	42.1
4/29/1991	375.6660	0.2635	-103.5	71.1		734.7964	0.1183	-70.5	49.1
	375.6951	0.2696	-102.5	74.1		734.8260	0.1245	-78.5	48.1
	375.7250	0.2758	-102.5	74.1		734.8558	0.1307	-79.5	52.1
	375.7549	0.2821	-102.5	70.1		734.8898	0.1378	-83.5	53.1
	375.7944	0.2903	-102.5	70.1	4/23/1992	735.7572	0.3186	-94.5	66.1
	375.8236	0.2964	-101.5	70.1		735.7919	0.3258	-93.5	64.1
	375.8528	0.3025	-98.5	70.1		735.8273	0.3332	-90.5	61.1
	375.8826	0.3087	-98.5	70.1		735.8565	0.3393	-89.5	60.1
	375.9118	0.3148	-97.5	66.1		735.8856	0.3453	-89.5	59.1
4/30/1991	376.6694	0.4727	-28.5	-8.9	4/24/1992	736.6745	0.5098	-7.5	-13.9
	376.6993	0.4789	-24.5	-8.9		736.7363	0.5227	0.5	-15.9
	376.7284	0.4850	-23.5	-8.9		736.7891	0.5337	5.5	-13.9
	376.7576	0.4911	-19.5	-11.9		736.8182	0.5397	9.5	-13.9
	376.8166	0.5034	-14.5	-12.9		736.8495	0.5463	11.5	-10.9
	376.8479	0.5099	-10.5	-12.9		736.8967	0.5561	18.5	-10.9
	376.8777	0.5161	-10.5	-16.9	4/25/1992	737.7633	0.7367	77.5	-95.9
	376.9194	0.5248	-1.5	-17.9		737.7911	0.7425	77.5	-95.9
5/01/1991	377.6805	0.6834	67.5	-97.9		737.8151	0.7475	77.5	-100.9

where $I_{RS\ CVn}$ is the normalized intensity in the spectrum of RS CVn at some wavelength point and $I_{Std}(RV)$ is the intensity at the same wavelength in the spectrum of a sharp-lined standard star shifted by radial velocity RV. The cross correlation is normalized to the number of points the two spectra have in common, N . The velocity shift for the maximum value of the cross correlation was taken as the radial velocity of the star. For the hotter component of RS CVn, we used α CMi (F5 IV) as the standard; for the cooler component, HR 5901 = κ CrB (K1 IV) rotationally broadened to 45 km s⁻¹. Figure 3 gives an example of the cross correlation between α CMi and a typical spectrum of RS CVn. The sharp maximum at 49 km s⁻¹ shift detects the hotter component; the cooler spotted component is the distorted profile near -70 km s⁻¹. Also shown in the figure is the cross correlation with the rotationally broadened spectrum of κ CrB. This shows how using an appropriate standard star can eliminate, to at least some extent, the distorting effects of the spots and how using a star with roughly the correct spectral type weights the cross corre-

lation function toward the desired component.

Radial velocities of the two standard stars were determined by cross correlating them with a large sample of bright stars of similar spectral types taken from the *Bright Star Catalogue*. We found radial velocities of -3.46 and -49.9 km s⁻¹, respectively, for α CMi and κ CrB, and we have corrected the velocities of the two components for these zero points.

Radial velocities derived for the two components are listed in Table 1 and are plotted in Fig. 4. We have assumed that the orbits of the two stars are circular and have fitted a sine curve to the radial velocities. Results are given in Table 2. Our fitting program lets us detect any shift of the phase of the sine curve from the phase of the light curve. This is seen in the phase of maximum velocity, θ_0 in Table 2; the values near 0.25 and 0.75 indicate there are no appreciable phase shifts. We give two sets of elements for the G-K cooler star. For the first, we have fitted all the radial velocities except for those in secondary minimum (phases 0.45-0.55), which are clearly affected by the

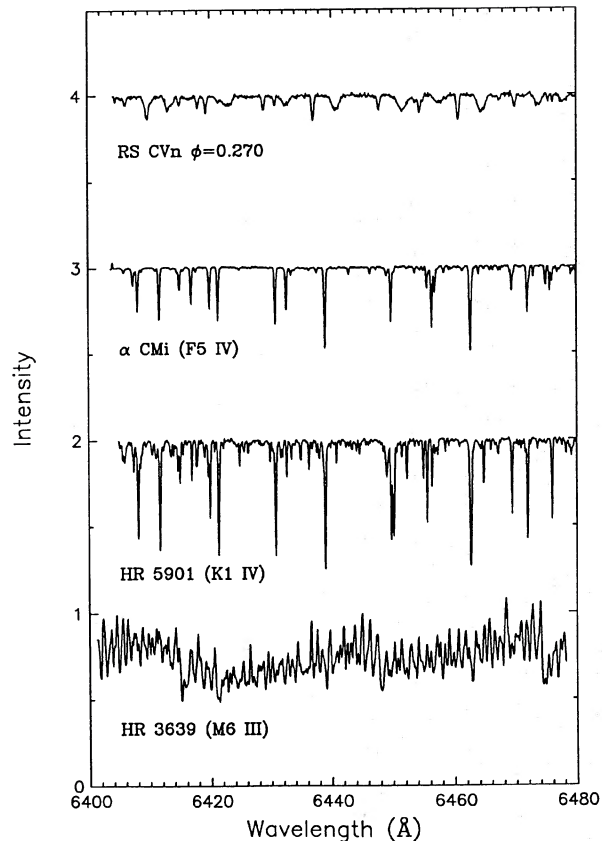


FIG. 2. Spectra of RS CVn and several comparison stars. The spectrum for RS CVn was taken at phase 0.270 in 1992. Spectra have been cleared of noise spikes and corrected for slopes in the continuum level. The bottom spectrum for HR 3639 (M6 III) represents a star only somewhat cooler than the spots are expected to be (3100–3400 K).

blending of the spectra. The second fit excludes not only the velocities for secondary eclipse but also the seven velocities in the phase range 0.6–0.8 that belong to two groups lying above the fitted curve, circled in the figure. This reduces the scatter about the fitted curve considerably and gives the two stars essentially the same average velocity. The amplitudes of the velocity curves agree very well with a previous study by Popper (1988), especially for the F star. For the G star, we find a somewhat lower amplitude, implying a bigger mass ratio, but the difference is no bigger than we find in our own data by excluding the outlying data. The cool star thus still appears to be a few percent more massive than the hot star, with the mass ratio, $M_c/M_h = 1.04 \pm 0.02$.

4. ANALYSIS OF LIGHT CURVES AND LINE PROFILES

We have used a computer model of the binary similar to the program of Kang & Wilson (1989) to fit the light curves. In it, the geometry of the binary is defined by the mass ratio, $q = M_c/M_h$, the orbital inclination, i , and the relative radii (side radii of an equipotential surface in the Roche model), $r = R/a$, where a is the semimajor axis of

the orbit. The surface brightness distribution in the absence of spots is determined by a limb-darkening coefficient, $x_\lambda = 0.71$, gravity-darkening exponent, $g = 0.25$, and bolometric albedo, $A_{\text{bol}} = 0.3$. Basic properties of the binary system are given in Table 3; the geometry comes from a combination of existing light-curve solutions (Eaton & Hall 1979; Kang & Wilson 1989), the mass ratio and semi-major axis come from the new radial-velocity solution, the limb-darkening coefficients are from model atmospheres, and the temperatures come from light-curve solutions. The model lets us put up to ten spots on the cool star, each bounded by great circles of longitude and small circles of latitude. Parameters defining each spot are its limits in latitude, β , its central longitude, λ , its extent in longitude, $\Delta\lambda$, and its effective temperature, T_{spot} . We take the longitude to increase in the direction of orbital motion from the line between the components. Thus the phase at which a spot is closest to disk center, ϕ_0 , is related to central longitude, λ , as

$$\phi_0 = 0.50 - \lambda/360. \quad (3)$$

Since we do not have infrared photometry for 1991 or 1992, we have assumed the spots are all at $T_{\text{spot}} = 3450$ K, as found for the dominant spots in 1984 (Eaton 1991). Because the spots can block light at all phases, we have normalized the calculated light to roughly the brightness the star would have at quadrature without any of the spots and multiplied by a constant (added a zero point on the magnitude scale) to fit the level of the observations.

Because the light-curve program divides the model star's surface into a discrete grid for the calculation (roughly $= 3.6 \times 2.3$ deg at the equator in longitude and latitude), the edges of the spots must conform to this division, as noted by Kang and Wilson. Our program therefore adjusts the edges of spots to coincide with the assumed grid, and this is the reason for the peculiar precision and quantization of spot properties reported in Tables 4 and 5.

Initially, we attempted to fit each light curve with at most two spots, inasmuch as Kang and Wilson had fit four light curves adequately with two spots each. This proved impossible, so we allowed three spots, getting the acceptable solutions shown in Fig. 1. These could have been improved slightly, if they had reproduced the observed line profiles. However, they did not.

We have also written a computer program that calculates the line profiles for the spot model. In this calculation, we assume that each visible point on the surface of a star has the spectrum of a star of the same spectral type. This spectrum is weighted by the projected area and surface brightness in the R band and Doppler shifted to the radial velocity of the point. We add up the contributions from all parts of the surface visible at a given phase to form a spectrum, then calculate its cross-correlation function with respect to κ CrB per Eq. (2) for comparison with the observations. For these calculations, we have used our spectrum of α CMi to represent the hot star and our spectrum of κ CrB to represent the cool star. We have also assumed the spots are black, which will change the result very little, inasmuch as the spectrum of a cool spot should

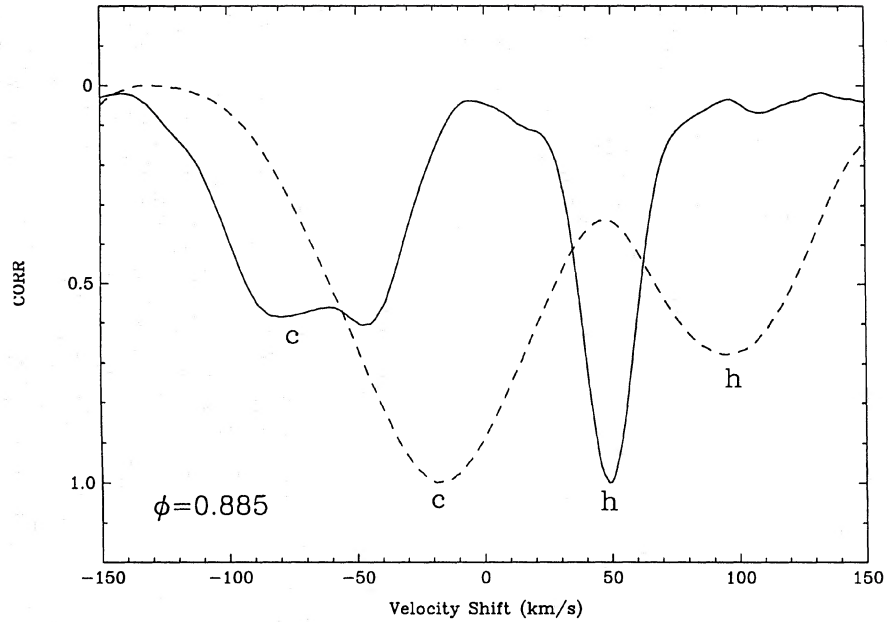


FIG. 3. Sample cross-correlation functions for RS CVn. A spectrum at phase 0.885 on 1992 April 20 has been cross correlated with spectra of α CMi (solid line) and κ CrB broadened to $v \sin i = 45 \text{ km s}^{-1}$ (dashed line). Signatures of the hot and cool components are marked below the cross-correlation functions. The solid curve shows the unmistakable signature of a spot near the center of the cool star's disk.

be very different than that of the surrounding photosphere (see Fig. 2) and because spots are less than $\sim 30\%$ as bright as the unspotted photosphere.

When we use this program to predict profiles for the spot solutions of Table 4, we find that the profiles are

wrong, that they do not fit the observations. Specifically, the spot depressing the light around phase 0.1 in 1992 predicts a much larger distortion in the line profiles than observed, and the observed line profiles require other spots, such as those distorting the line profiles at phase 0.70 in

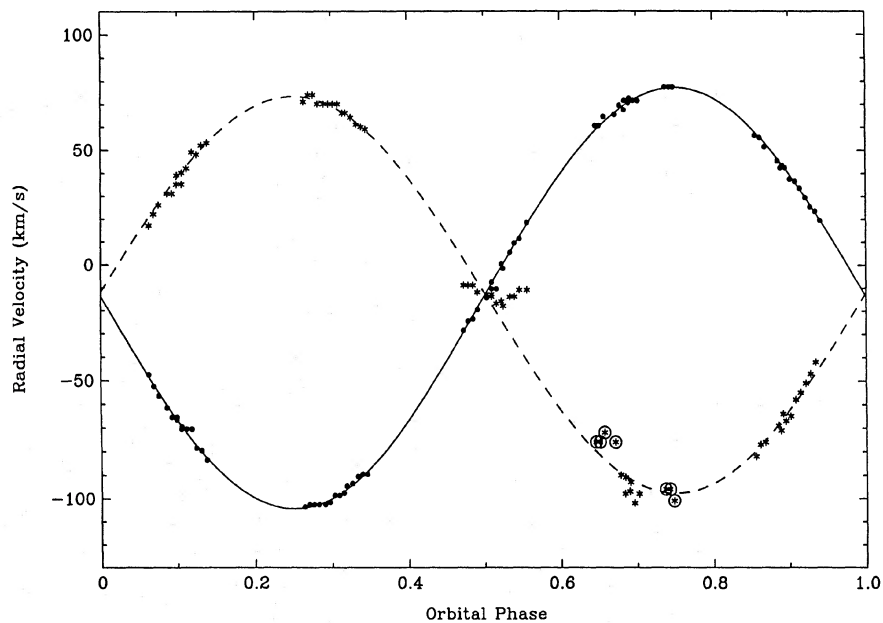


FIG. 4. Velocity curves for the F5 star (dots) and G8 stars (asterisks) derived from the 70 NSO spectra. Curves represent circular orbits with properties given in Table 2. Those data outside secondary eclipse that were excluded from the adopted solution are circled.

TABLE 2. Radial-velocity solutions.

Quantity	F Star ^a	G-K Star	G-K Star ^a	Popper (1988)
K (km s ⁻¹)	-90.71 ±.36	85.55 ±.65	86.90 ±.52	-90.4/88.5
γ (km s ⁻¹)	-13.59 ±.19	-12.11 ±.53	-13.49 ±.45	-14
No. points	70	55	48	-
σ (km s ⁻¹)	1.6	3.7	2.7	-
θ ₀ (phase)	0.2502	0.7519	0.7484	-
q = M _c /M _h		1.060	1.044	1.02

Footnote: a. Adopted solution.

TABLE 3. Properties of the RS CVn system.

Quantity	F Star	G-K Star
q = M _K /M _F		1.04
i (deg)		85.55
r/a	0.1152	0.2466
a (R _⊙)		16.9
M (M _⊙)	1.37	1.44
x _V	0.55	0.71
T _{phot} (K)	6800	4580
T _{spot} (K)	-	3450

TABLE 4. Three-spot solutions of light curves.

Spot No.	β	1991		β	1992	
		λ	Δλ		λ	Δλ
1	-9.2 to +9.2	75.6	28.8	-16.3 to +16.3	118.8	46.8
2	-9.2 to +9.2	180.0	21.6	-13.9 to +13.9	208.8	39.6
3	-16.3 to +16.3	291.6	36.0	-16.3 to 0.0	334.8	28.8

Note: The β values are limits to the spot in latitude, λ is the central longitude, and Δλ is the width of the spot in longitude. Zero points for the two years are ΔV = -0.335 and -0.360, respectively.

TABLE 5. Final multispot solutions.

Spot No.	β	1991		β	1992	
		λ	Δλ		λ	Δλ
1	-9.2 to +6.9	10.8	21.6	-6.9 to +6.9	57.6	25.2
2	+16.3 to +39.6	32.4	28.8	-11.5 to +11.5	104.4	36.0
3	-13.9 to +13.9	90.0	28.8	-13.9 to +13.9	144.0	32.4
4	-9.2 to +9.2	147.6	36.0	-11.5 to +11.5	212.4	39.6
5	+9.2 to +28.7	212.4	18.0	-9.2 to +9.2	262.8	25.2
6	-11.5 to +11.5	244.8	21.6	-16.3 to +0.0	324.0	28.8
7	-16.3 to +16.3	288.0	25.2			
8	-9.2 to +16.3	320.4	25.2			

Note: See Table 4 for a definition of parameters. Zero points for the two years were both ΔV = -0.370.

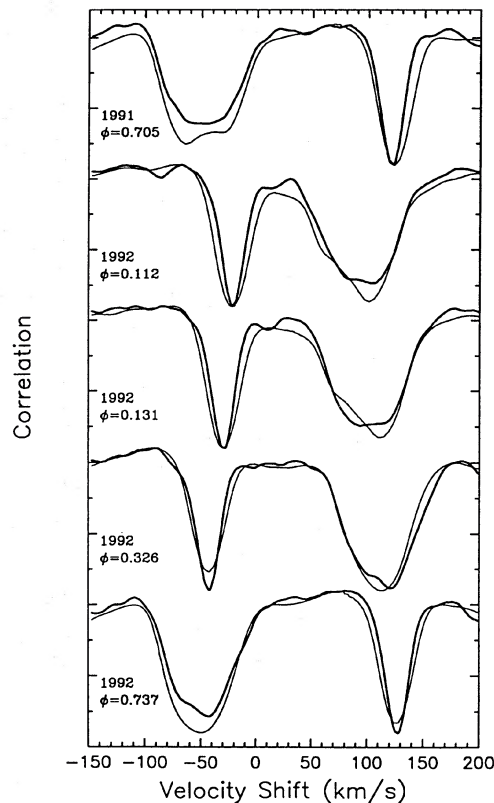


FIG. 5. Sample line profiles (cross-correlation functions) for the three-spot solutions. These cross-correlation functions have been renormalized to make them range between 0.0 and 1.0; thin curves represent the calculation, and heavy curves, the observations. We chose the phase illustrated because they represent failures of the three-spot solutions. In the top three panels, the spot signature in the calculation is much too strong, which indicates the single spots producing it are much too big. In the lower two panels, we have phases when line-profile distortions detect a spot but none is seen in the three-spot solution.

1991 and phases 0.33 and 0.73 in 1992, that were not required by the photometry. Figure 5 illustrates the difference between observed cross-correlation functions and those calculated for the three-spot model.

We next tried to fit the light curves for the two years with the same photometric zero points, using only spots to change the shape and mean level of the light curve and to fit the line-profile distortions. We have accomplished this with the set of spots identified in Table 5. Plots of the light curves are shown in Figs. 6 and 7. Correspondence between observed and calculated cross-correlation functions is shown in Fig. 8.

5. DISCUSSION

5.1 Use of Cross-Correlation Functions

The application of cross correlations to spotted stars was pioneered by Dempsey *et al.* (1992), who provide a much more antiseptic application than ours. They calculated cross-correlation functions for the two noneclipsing,

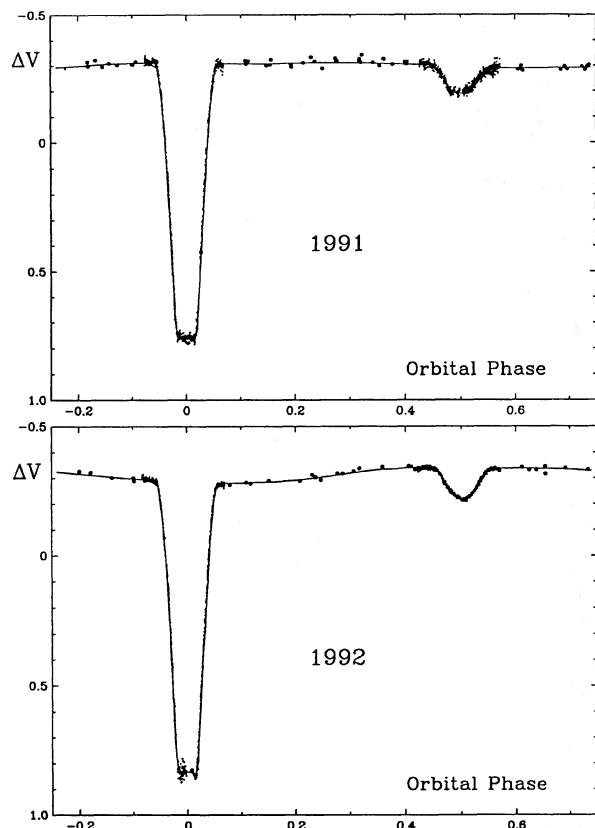


FIG. 6. Light curves for the final, multiple-spot solutions of Table 5.

rapidly rotating, highly spotted stars V711 Tau and HD 199178, after removing obvious lines of the second component and restricting themselves to wavelengths without any telluric lines. They argued that these precautions are necessary because the different spectrum of lines of a second component will introduce noise into cross-correlation functions, which can give apparent shifts in the phasing of spots. The uncorrelated telluric lines will lead to similar problems. The effect of secondary lines illustrated by Dempsey *et al.* is a slope of the central portion of the cross-correlation function (see their Fig. 1), which is equivalent to an apparent phase shift for the spot.

Because of the stronger blending in the spectrum of RS CVn, removing the second spectrum is impracticable. In fact, the strength of this method is that it allows highly blended spectra to be decomposed into their separate components. To assess the importance of such blending, we have calculated the cross-correlation function for all the observed spectra with respect to both α CMi and κ CrB. The cross-correlation functions showed the same distortions for both of these masks, even though their spectral types differed by more than a full class, although we do notice between them both differences in slope of the type identified by Dempsey *et al.* and differences in the sharpness of the spot signature. For this reason we feel the fits between observed and calculated cross-correlation func-

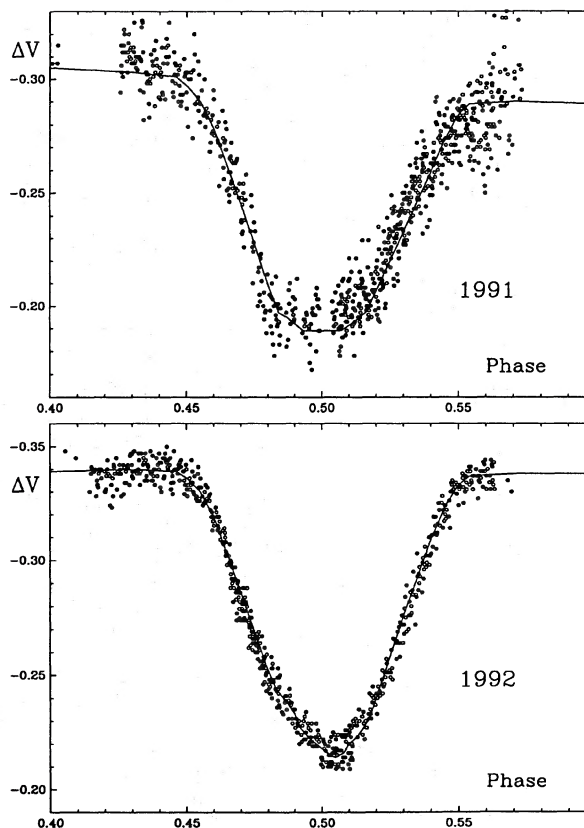


FIG. 7. Plots of the secondary eclipses for the final, multiple-spot solutions. These are highly sensitive to eclipses of spots. In fact, the solution for 1992, which detects the eclipse of the moderately sized spot at $\lambda = 324$ deg, is as good as can be expected of this type of analysis. The solution for 1991 involves eclipses of several spots, which make the calculated curve both narrow and shallow enough to fit the data. It could probably be improved somewhat by changing the spot distribution, but we have not done so because the large number of spots visible at this phase makes the solution uncertain. Also note that these curves are slightly variable over the time it took to collect the data. The eclipse shape in 1992 changed slightly between the second and third night of observation in a way suggesting a slight migration of the eclipsed spot in longitude.

tions, such as that for phase 0.671 in 1991, are as close as can be expected of this method.

The other source of noise in cross-correlation functions identified by Dempsey *et al.* is telluric lines, some of which affect the red end of our wavelength range. This should not have been especially bad for us, since we took all of the spectra in April, when the humidity was low. We have tested the effect of the few telluric lines included by calculating cross-correlation functions for spectra of θ CrB (B6 V) and γ Crv (B8 III) taken in 1992 April. These two stars have no intrinsic lines but show four noticeable telluric lines longward of 6470 \AA . The cross-correlation functions for them showed fluctuations at $\sim 10\%$ of the minimum level in cross-correlation functions of RS CVn. When we recomputed the cross correlations for $6400\text{--}6470 \text{ \AA}$, which excludes the detectable telluric lines, they changed very little, which shows that telluric lines were not a significant source of noise in our analysis.

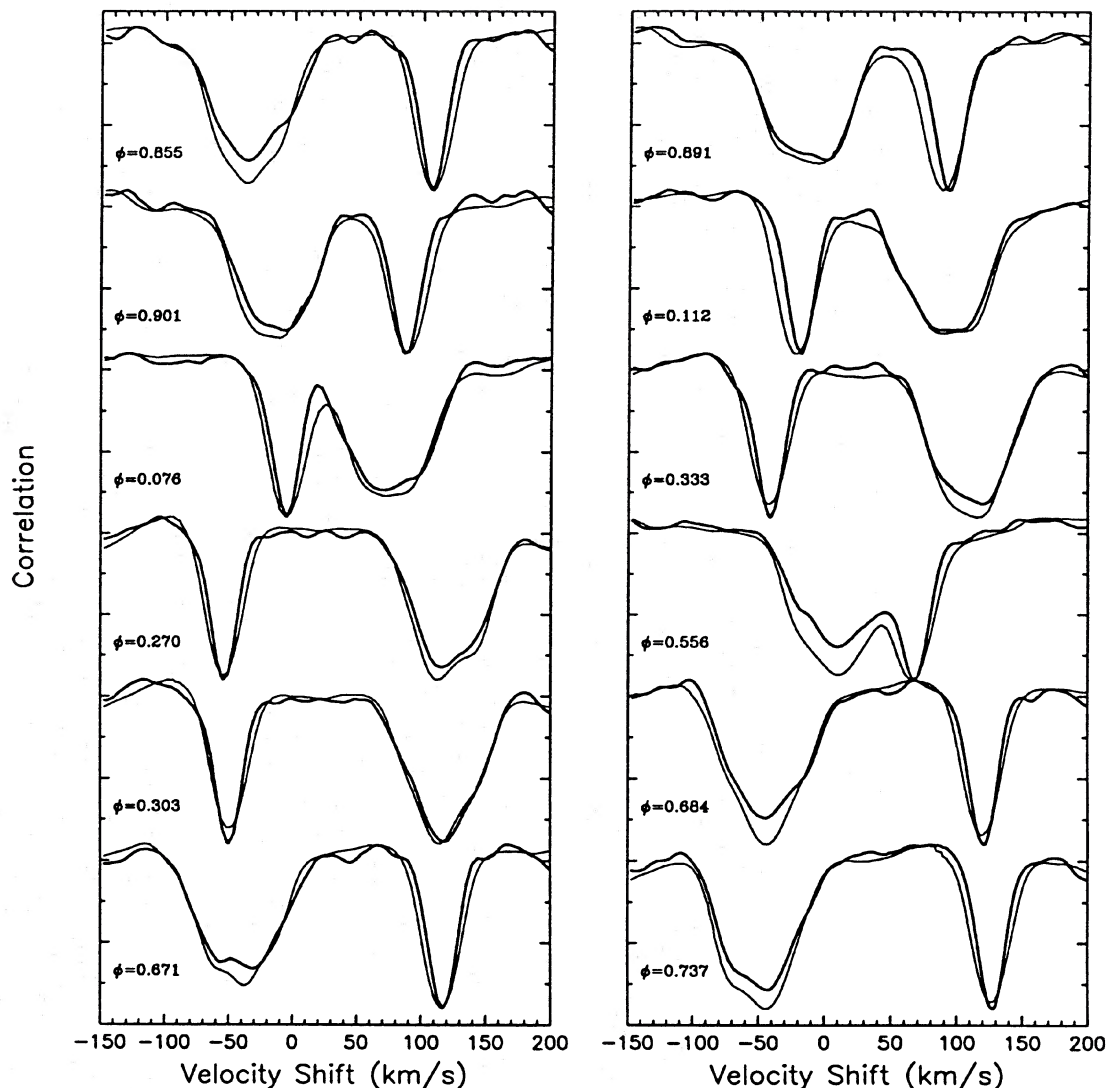


FIG. 8. Sample cross-correlation functions for the adopted multiple-spot solutions, 1991 to the left and 1992 to the right. All of these show the same sort of distortions in the calculations for our spot models as in the observations. Slight deviations from the observed cross-correlation functions cannot be considered significant, since this effect can result from blending with the spectrum of the second star (e.g., Dempsey *et al.* 1992).

5.2 Polar Spots?

We may ask whether there is any indication of polar spots in this system. Two lines of evidence may suggest them—the rotational velocity of the hotter component and the relatively high temperature of this hotter star.

One may have noticed the discrepancy between observed and calculated widths of cross-correlation functions for the hotter star in Figs. 5 and 8. The calculated curves are broader than the observed curve, and this implies that $v \sin i$ is less than expected of differential rotation. Strassmeier & Fekel (1990) have interpreted this effect as one-half synchronous rotation ($v \sin i = 11$ vs 21 km s^{-1}), but it could also result from overestimating the relative radius of the hotter star. To fit the width of the cross-correlation function, we would have to reduce the relative radius from

0.11 to around 0.08, not quite by a factor of two, but a very significant change for the light-curve solution. The radius of the cool star would adjust slightly and the inclination would be reduced to give the observed duration of total eclipse. The effect of this change in ratio of radii is to make the cool star far too luminous to preserve the eclipse depths. Perhaps its luminosity could be reduced by large polar spots? This, however, would require spots extending from the poles to latitudes ± 16 degrees, covering about 72% of the cool star's surface. These are not allowed by the line profiles.

We would expect an effective temperature near 6400 K for an F6 star, not the 6800 K we have used to fit the eclipse depths. There is a difference of about 0.28 mag in the visual surface brightness between these two tempera-

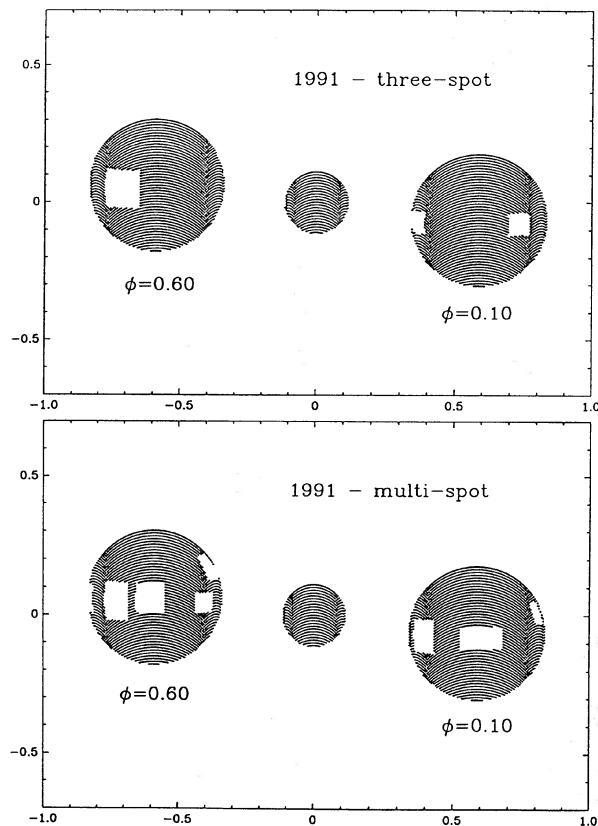


FIG. 9. Maps comparing the three-spot and eight-spot solutions for 1991 for phases one-half cycle apart. When the distributions are compared, there are obvious similarities but definite differences.

tures (Eaton & Poe 1984). Fitting the light curves would require a 24% reduction in the apparent luminosity of the spotted star, were we to reduce T_h this much. If this reduction were caused by polar spots, they would have to extend from the poles to latitudes ± 35 deg. More likely reasons for the higher temperature of the hot star are that we used the larger radius of Kang and Wilson for the cooler star (0.2466 vs 0.235 of Eaton and Hall), which requires a somewhat higher T_h , that we have raised T_h too much to keep T_c from dropping much below 4600 K, and that there is a systematic error in the spectral types of Strassmeier and Fekel. Strassmeier and Fekel found that the cooler component is about 15% brighter than the hot component at 6400 Å, while the light-curve solutions, specifically those based on *VRI* photometry (Eaton 1991), predict it should be 5%–30% fainter. This argues for a hotter F star with intrinsically weaker lines, as well as for stronger lines in the cool star's spectrum than found by Strassmeier and Fekel.

The calculated line profiles for either of these sets of polar spots would also be far different than the observed profiles. Spots extending from the poles even to 64 degrees, which cover 10% of the star's whole surface, would give a large hump in the middle of line profiles, bigger than any of the distortions illustrated in Figs. 5 and 8. Even a pair of

spots extending only 18 degrees from the poles, covering 5% of the star's surface, would produce a permanent feature in line profiles comparable to those spot distortions seen in our spectra. In fact, the profiles calculated without any polar spots at all (cf. Fig. 8) seem capable of reproducing the observed line shapes. So we see no compelling evidence for very large polar spots in RS CVn, and the line profiles argue for polar spots even smaller than ~ 18 deg radius.

5.3 Numbers and Sizes of Spots

Our analysis of RS CVn finds many more spots than would be expected for our previous understanding of highly spotted chromospherically active binary systems. It may not be clear that all these small spots must actually exist. However, if spots truly account for the light-curve distortions, at least *one* of them has moderate properties. This is the spot eclipsed in 1992 (no. 3 in Table 4 and no. 6 in Table 5), which causes the pronounced distortion of secondary eclipse. The other spots detected spectroscopically in these years are also moderately sized, as well. The large (32×47 deg) spot that depresses the light near phase 0.1 in the three-spot solution for 1992 is inconsistent with line profiles. Instead, it must break up into at least two moderate-sized spots (nos. 2 and 3 in Table 5), or be a spot much broader in longitude than tall in latitude, to fit the line profiles. The many spots seen near phase 0.5 ($\lambda \sim 0$) in 1991, likewise, might seem to be a fanciful interpretation of the data. However, some distribution of spots like them is needed to fit the shape and level of secondary eclipse in 1991. This is a difficult eclipse to fit. It seems symmetrical and thus not obviously distorted by spots, yet the depth is less than it would be without spots. A spot centered near phase 0.68 (no. 7) is needed to give observed line-profile distortions as well as to produce the obvious depression of the light near phase 0.7. But this spot cannot be big enough to give the full depression. Rather, spot no. 8, at such a high latitude that it is only partially eclipsed, must contribute. Spot no. 1, specifically, is needed to give the right depth and duration of secondary minimum.

We have been unable to restrict the *latitudes* of the spots effectively because noise in the cross-correlation functions and spectra limit our ability to detect spot effects to times when the spots are near the center of the star's disk. Effects in the line wings, which are needed to determine how far a spot gets from the center of the star's disk, are below our limit of detection. Some spots, such as no. 5 of 1991, work better if moved away from the equator, but they are the exception. Likewise, spot 6 in 1992 probably must be somewhat below the equator for it to be eclipsed so completely. The shapes of individual spots are also largely indeterminate, although in a few cases we can tell that what would at first appear to be large single spots are really groups of spots spread out in longitude, or they are single spots much broader in longitude than tall in latitude. Even with the small spot sizes we infer, a few features in the line profiles seem to require even smaller, more complex groups of spots. An example of this is the spot distorting the profile

of phase 0.076 in 1991, which does not reproduce all of the structure in the profile illustrated. Another is the spot eclipsed in 1992, which distorts the red edge of the profile at phase 0.684. This profile would fit much better if the spot extended to somewhat smaller longitude, which probably requires it to break up into two parts.

One further line of evidence that these stars have many moderately sized equatorial spots is that the three-spot solutions require different luminosities for the two years while the multispot solutions do not. The 0.025 mag shift in photometric zero point between 1991 and 1992 in Table 4, which contrasts with the estimated maximum change of ± 0.01 mag in the photometric system between the years, implies that *both* stars got brighter. This seems exceedingly unlikely. The physical solution in Table 5 does not need this change, for it accounts for the changes in mean level entirely with those spots on the cooler star needed to fit line profiles.

6. SUMMARY

We have begun to resolve the distribution of spots in RS CVn with a combination of photometry and high-dispersion spectroscopy. Crude maps of the surface are given in Figs. 9 and 10. They show what appear to be spots of typically $\Delta\beta \times \Delta\lambda = 22 \times 28$ deg spread over the surface of the star. The most noticeable property of these diagrams is the way large single spots tend to break up into pairs of smaller spots with the added resolution afforded by spectra. There may be a suggestion of bipolar spots, but the resolution is not high enough to tell. The spot eclipsed in 1992, with potentially the highest resolution, need not be bipolar. And, yet, there is a suggestion in the line profile for phase 0.684 that it extends to smaller longitude than in our model. There is little evidence for polar spots larger than ~ 18 degrees in radius. This limit is only slightly bigger ($r=18$ vs 14 deg) than the moderate spots we have found at lower latitude.

REFERENCES

- Dempsey, R. C., Bopp, B. W., Strassmeier, K. G., Grados, A. F., Henry, G. W., & Hall, D. S. 1992, *ApJ*, 392, 187
- Eaton, J. A. 1991, in *Surface Inhomogeneities in Late-Type Stars*, edited by P. Byrne and D. Mullan (Springer, Berlin), p. 15
- Eaton, J. A., & Hall, D. S. 1979, *ApJ*, 227, 907
- Eaton, J. A., & Poe, C. H. 1984, *AcA*, 34, 97
- Genet, R. M., Boyd, L. J., Kissell, K. E., Crawford, D. L., Hall, D. S., Hayes, D. S., & Baliunas, S. L. 1987, *PASP*, 99, 660
- Hall, D. S. 1976, in *Multiple Periodic Variable Stars, Part I*, IAU Colloquium No. 29, edited by W. S. Fitch (Reidel, Dordrecht), p. 287
- Hall, D. S., & Henry, G. W. 1993, in *Proc. of the Workshop on Robotic Telescopes*, Kilkenny, Ireland, edited by B. P. Hine and M. F. Bode (in press)
- Henry, G. W., Eaton, J. A., Hamer, J., Nagarajan, R., & Hall, D. S. 1993, *ApJ*, in preparation
- Henry, G. W., & Hall, D. S. 1993, in *Proc. of the Workshop on Robotic Telescopes*, Kilkenny, Ireland, edited by B. P. Hine and M. F. Bode (in press)
- Kang, Y. W., & Wilson, R. E. 1989, *AJ*, 97, 848
- Noah, P. V., Bopp, B. W., & Fekel, Jr., F. 1987, in *Cool Stars, Stellar Systems, and the Sun*, edited by J. L. Linsky and R. E. Stencel (Springer, Berlin), p. 506
- Popper, D. M. 1988, *AJ*, 95, 1242
- Ramsay, L. W., & Nations, H. L. 1980, *ApJ*, 239, L121
- Strassmeier, K. G., & Fekel, F. C. 1990, *A&A*, 230, 389
- Strassmeier, K. G., Hall, D. S., Zeilik, M., Nelson, E., Eker, Z., & Fekel, F. C. 1988, *A&AS*, 72, 291
- Vogt, S. S., & Penrod, G. D. 1993, *PASP*, 95, 565

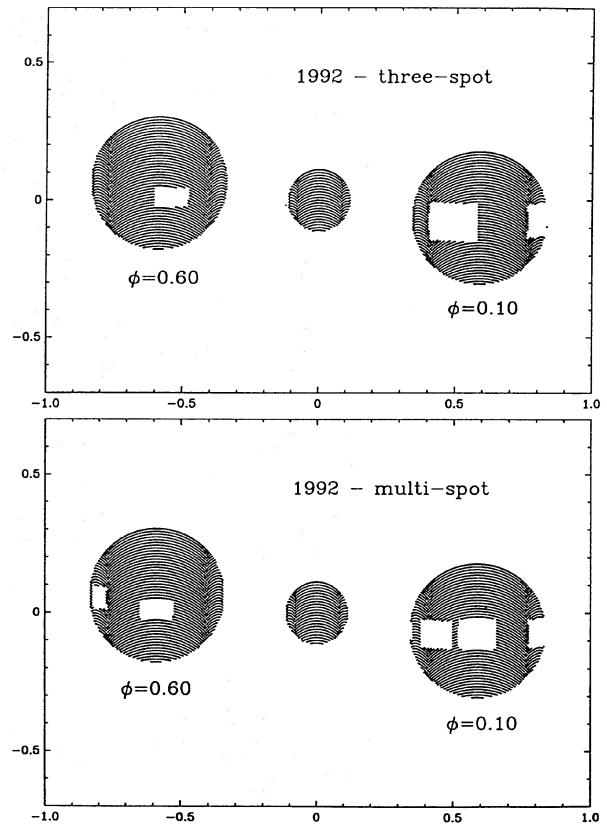


FIG. 10. Maps comparing the three-spot and six-spot solutions for 1992.

We would like to thank the staff of the National Solar Observatory for help with planning and taking the observations. This research has been supported by NASA Grant No. NAG 8-111 for operating the robotic telescope and NSF Grant No. HRD 9104484 for the analysis.